

DRAINAGE DENSITY AND VALLEY EROSION INDEX AT DEEP-SEATED LANDSLIDES IN THE CENTRAL KII MOUNTAINS, SOUTHWEST JAPAN

Muneki Mitamura¹ and Kazuma Kasahara¹

¹Geosciences, Osaka City University
3-3-138 Sugimoto, Sumiyoshi, Osaka 558-8585, Japan
Email: mitamura@osaka-cu.ac.jp

ABSTRACT

The central part of the Kii Peninsula is a mountainous area composed of Cretaceous accretionary prisms with undulations of about 1000 m. Many mountain slopes have gravitational rock creep. The heavy rains of the Typhoon Talas (2011) caused many deep-seated landslides. Most of the landslide slopes are dip slopes facing northwest. This typhoon moved slowly, causing continuous rainfall of 20-40 mm/hour, with total rainfall of over 800 mm for five days in this area. It is clear that rainwater infiltration has led to destabilization of mountain slopes, and it is important to evaluate the hydraulic properties of mountain slopes. Therefore, using 5 m DEM data measured before 2011, we evaluated the drainage density and valley undulations, which are indicators related to rainwater infiltration on rock creep slopes.

The drainage density was calculated by dividing the valley length by the dimensions of the tributary catchment extracted on QGIS using 5 m DEM. Two-dimensional wavelet analysis using a Mexican Hat filter was performed to evaluate the degree of valley erosion. Since the convolution integration is performed for a 5 m DEM with a filter size of 9×9 , the undulations of the representative wavelength of 20 m of the terrain are evaluated.

As a result of examining the target area of 10 km square, the drainage density is relatively low on the northwestern slope, which is a dip slope, and among them, the landslide traced areas tends to be low. Valleys with a negative wavelet coefficient close to zero using the Mexican Hat filter have a small degree of erosion, and are evaluated as shallow. Comparing the wavelet coefficient distributions of the entire area and the landslide area, it was found that the proportion of shallow valleys with a coefficient of less than 0 to -5 or more is predominant in the landslide area. The small drainage density and the predominance of shallow valleys in the landslide area suggest that no significant surface water is produced in those drainage areas. Opposite slopes tend to have high valley densities, and many surface collapses are observed, but few lead to deep-seated landslides. Therefore, it was clarified by DEM analysis that bedrocks in the dip slope is loosened by rock creep and is prone to rainwater infiltration. It can be seen that such slopes tend to lead to deep-seated landslides.

1. INTRODUCTION

Typhoon Talas (2011) passed through the west Japan from 30th August to 4th September 2011 (Japan Meteorological Agency, 2013). This typhoon led to the heavy rain record that the total precipitation for 5 days in the southeastern part of the Kii Peninsula more than 1000 mm. The maximum record was 1652 mm for 72 hours and total precipitation of 1814 mm at Kami-kitayama Village, Nara. This total precipitation for 5 days is roughly equivalent to the annual rainfall average of Japan and 60% of the annual rainfall in this area.

Deep-seated landslides more than 10,000 m² in area have been confirmed 54 locations by Nara Prefecture (Figure 1). 13 sites of these large scale landslides induced natural damming of river channels with debris deposits (Kinki Regional Development Bureau, Ministry of Land, Infrastructure and Transport, 2013). These landslides mostly occurred in dip slopes consisting of the Cretaceous accretionary complex of the Shimanto Group (Kishu

Shimanto Research Group, 2012).

It is clear that rainwater infiltration has led to destabilization of mountain slopes, and it is important to evaluate the hydraulic properties of mountain slopes. Therefore, using 5 m DEM data measured before 2011, we evaluated the drainage density and valley undulations, which are indicators related to rainwater infiltration on rock creep slopes.

2. GEOLOGICAL SETTING

The 10 km square research area is located in the central part of the Kii Mountains, where the main stream and tributaries of the Totsukawa River flow, forming a canyon with undulations over 500m.

Deep-seated landslides mainly occurred in the Cretaceous accretionary complex of Shimanto Group (Kishu Shimanto Research Group, 2012). Oceanic and terrigenous facies are alternated in each tectonostratigraphic unit consisting of several thrust sheets. The oceanic facies intercalated in the lower part of thrust sheet is well sheared, and formed the tectonic mélange. The shear deformation is stronger in the older complex units located in northern part of the Shimanto Group terrain. The basal shear plane of large scale landslide is mainly formed in the lower part of the thrust sheet consisting of muddy tectonic mélange zone. Because thrust sheets generally incline toward north or northwest in this area, north or north western slopes are in the dip slope situation. Almost deep-seated landslides are occurred in dip slope areas (Figure 2).

3. DEM DATA AND ANALYTICAL METHODS

The DEM dataset which was provided by the Kinki Regional Development Bureau, is 5 meter intervals ground elevation data which records the pre-disaster terrain by airborne LiDAR in 2010. The former topography of the deep-seated landslide in 2011 can be evaluated with this data set. We selected and analyzed a data set of about 10 km square in a mountainous area where major collapses occurred frequently (Figures 1, 2). National Research Institute for Earth Science and Disaster Prevention, Japan (NIED, 2005) published the digital archive for landslide distribution maps. NIED detected topographical traces formed by landslide movement with 1970s aerial photographs on an approximate 1:40,000 scale.

The analysis work was done using QGIS. The valley lines were extracted by the method using the Median Filter of Iwahashi (1994). The tributary catchment area was extracted using “r.watershed” tool, which is one of the GRASS raster tools under 500 meshes of minimum size of exterior watershed basin. The drainage density was calculated by dividing the valley length by the dimensions of each tributary catchment area. Valley reliefs were carried out using a 2D wavelet analysis with a 9×9 Mexican Hat digital filter (Booth *et al.*, 2009; Fujisawa and Kasai, 2009). Since a 5 m DEM set is used, evaluation will be

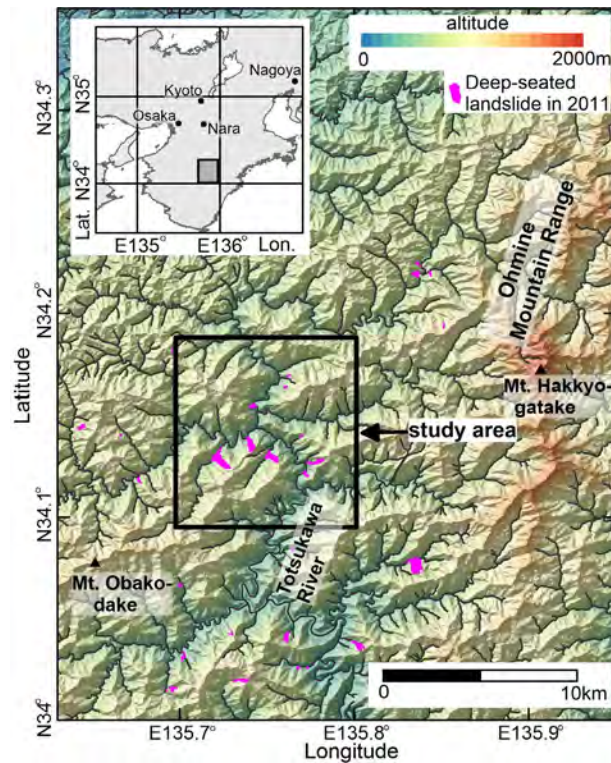


Figure 1. Location map of study area

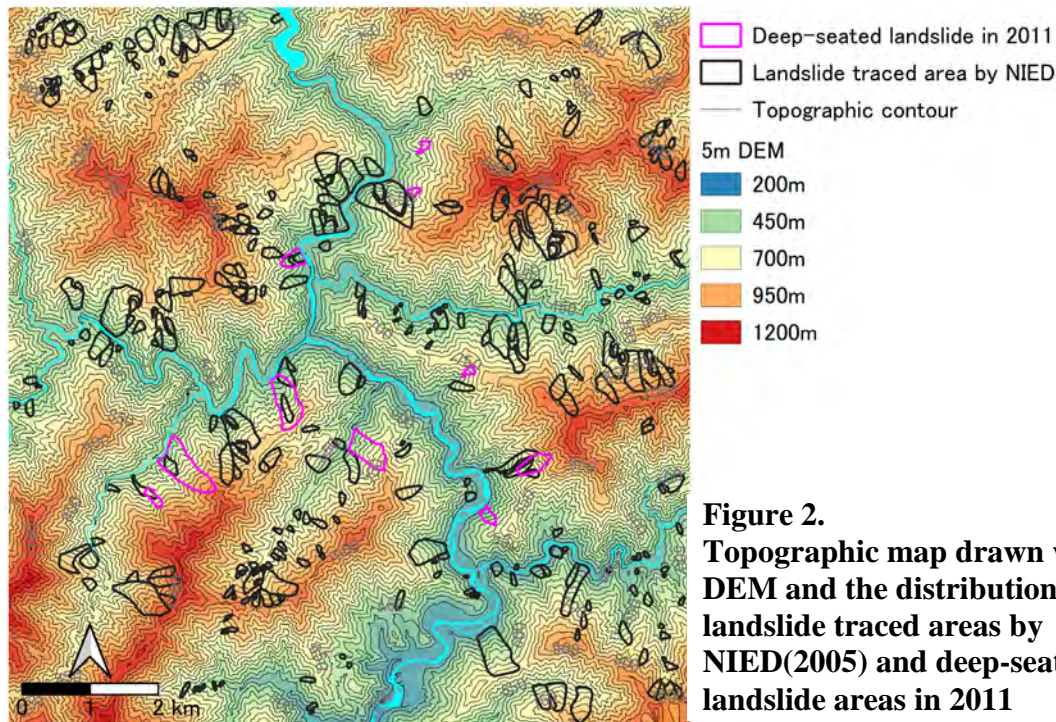


Figure 2.
Topographic map drawn with 5m DEM and the distribution of landslide traced areas by NIED(2005) and deep-seated landslide areas in 2011

performed for reliefs of representative wavelength 20 m. The results of the 2D wavelet analysis were statistically evaluated in tributary catchment areas and landslide areas.

4. RESULTS

4.1 Drainage density

Detected tributary catchment areas are 3570 plots, and the range of those dimensions are from 2 to 8 ha. The drainage density shows a distribution with an average of 26.2 km^{-1} and a standard deviation of 7.6 km^{-1} . Figure 3 shows the distribution of valley densities in different colors. Most of the major ridge lines which are shown by hatched lines in Figure 3, extend NE-SW direction. It can be seen that the drainage density of the tributary catchment area on the northwestern slope of the main ridge line is smaller than that on the southeastern slope. There are many landslide traces on the NIED landslide map on the northwestern slope, and deep-seated landslides have also occurred. Valley densities are rated low in most of these areas.

4.2 Valley Relief

Figure 4 shows the distribution of wavelet coefficients evaluated by the Mexican Hat digital filter. The distribution of wavelet coefficients indicates that the ridges with large positive values and valleys with significant negative values are repeated on the southeast side slopes of the main ridge line, and those slopes is rich in undulations. On the other hand, the northern or western slopes of the major ridge lines have low undulations and valleys in those areas are poorly developed.

5. DISCUSSION

5.1 Valley Erosion Index

The distribution of wavelet coefficients indicates poor valley development on the

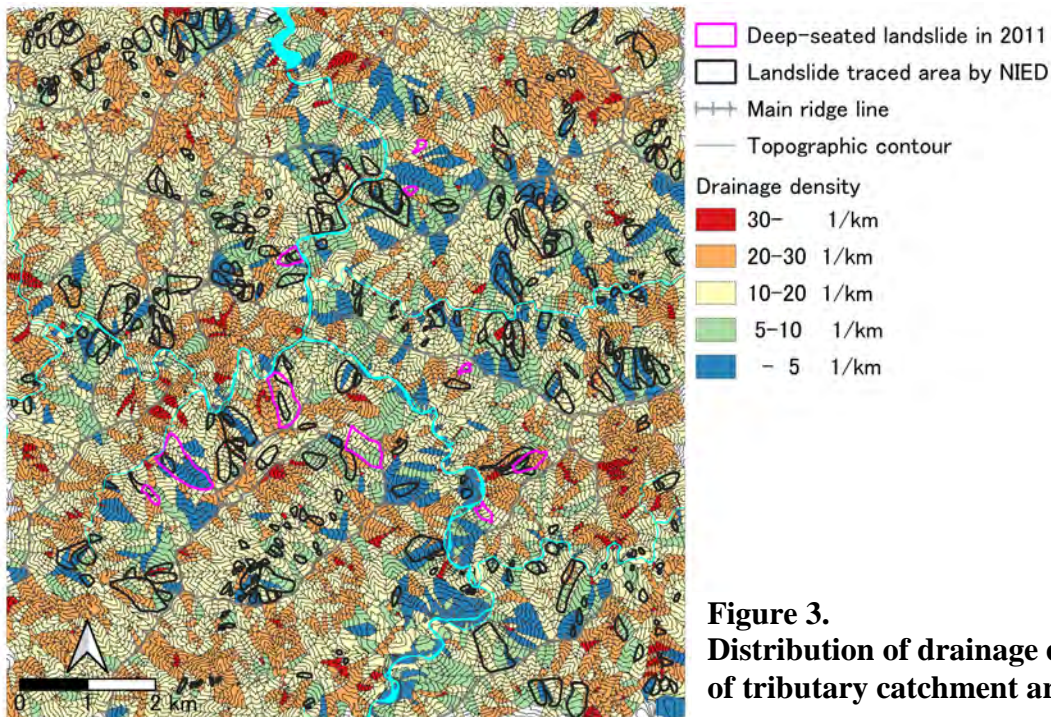


Figure 3.
Distribution of drainage density of tributary catchment area

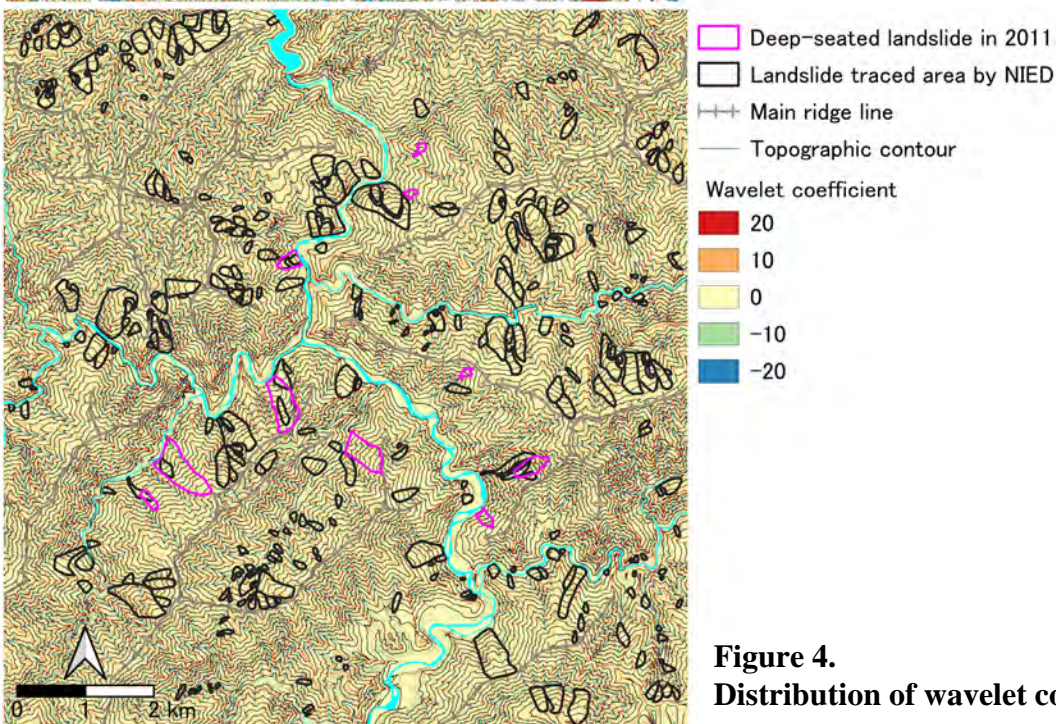


Figure 4.
Distribution of wavelet coefficient

northwest side of the main ridge line. We compared the distribution statistics of wavelet coefficients along the valley line in the entire survey area and the landslide area. Figure 5 shows the distribution of wavelet coefficients in each area. There is a difference in the distribution between the wavelet coefficients value range of -5 to less than 0 and the range of -20 to -10. In landslide areas, the proportions in the wavelet coefficients value range of -5 to less than 0 are predominant. While, in the range of -20 to -10, the distribution ratio of landslide traced area is relatively low. The former topography of deep-seated landslide areas has a similar tendency.

Therefore, the ratio of the range of -20 to -10 to the range of -5 to less than 0 was evaluated as the valley erosion index in each landslide traced area. A small value of the

valley erosion index indicates that the valley development is poor. Almost valley erosion indexes in landslide traced areas and the former topography of deep-seated landslide areas are less than 1 (Figure 6).

5.2 Rock Sliding and Valley Development

The northeast-southwest direction of the main ridge lines corresponds to the strike direction of the main geological structure in this area. Since the main inclination direction of the Shimanto accretionary prism in this area is north or northwest, the northwestern region to the main ridge line is in a dip slope. As shown in Figure 2, it is clear that the drainage density of the tributary catchment area in this region tends to be small. The low drainage density region suggests the situation of significant infiltration of rain water (Horton, 1945). Dip slopes are prone to rock sliding from deeper positions, destabilizing the slopes. Instability of the slope leads to the formation of cracks in the bedrock and promotes rainwater infiltration. As a result, those situations are reflected in the topographical characteristics of small drainage density. The small valley erosion index also shows poor valley development, suggesting a situation where surface water erosion of the valley is small. Almost these indexes at landslide traced areas and former topography of deep-seated landslide areas are small. Therefore, the small drainage density and the small valley erosion index in this area can be one of effective indicators of the destabilizing area.

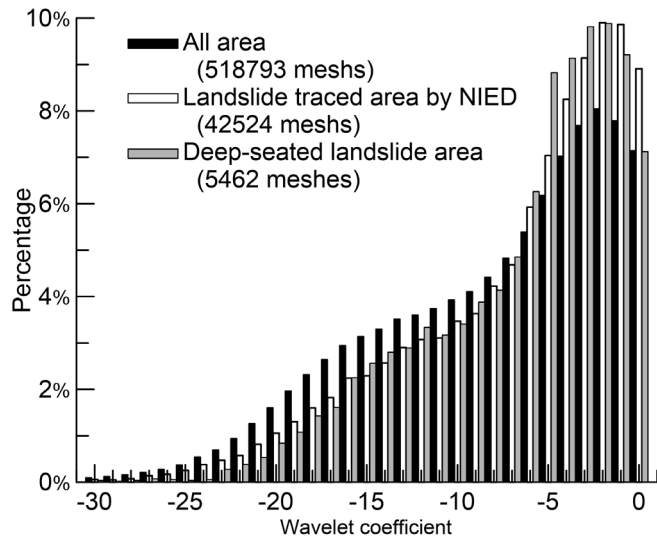


Figure 5.
Comparison of wavelet coefficient histograms among all areas and landslide areas

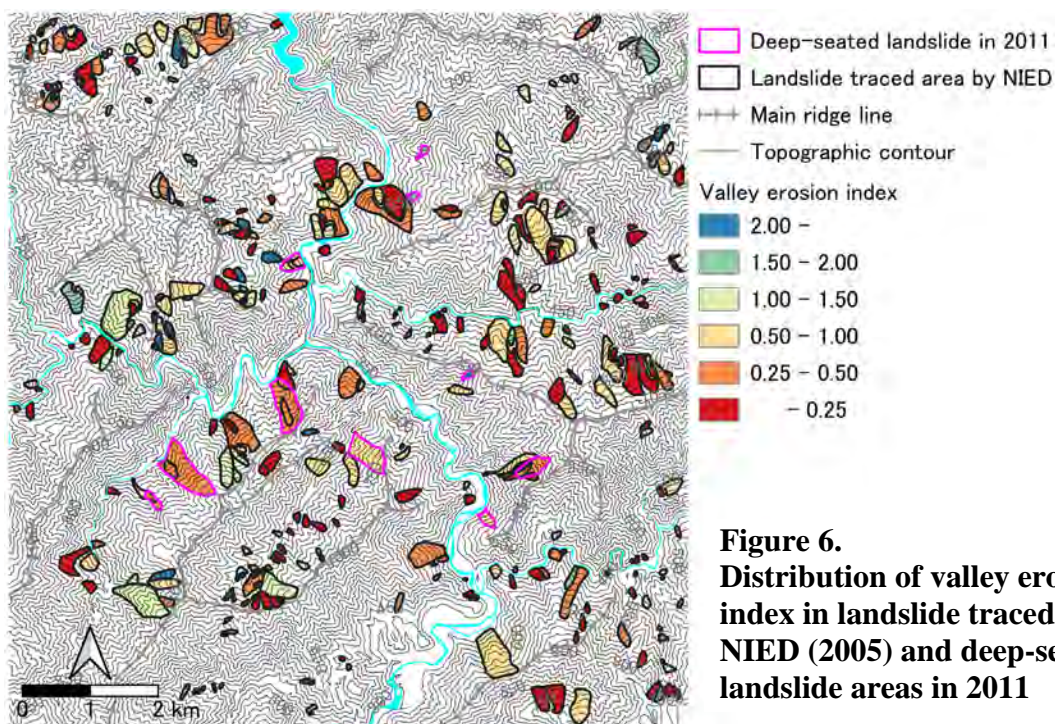


Figure 6.
Distribution of valley erosion index in landslide traced areas by NIED (2005) and deep-seated landslide areas in 2011

5. CONCLUSION

Using 5m DEM data before the occurrence of a large-scale heavy rain disaster, we evaluated the drainage density related to rainwater infiltration in the landslide traced area and the occurrence area of deep seated landslide area mountain slopes composed of Cretaceous accretionary prisms. The drainage density in the dip slope area was relatively low, and the evaluation was also low in the landslide area. The newly devised valley erosion index, which is the distribution ratio on wavelet coefficients of -20 to -10 to the range of -5 to less than 0, also shows a tendency similar to drainage density.

DEM analysis clarified that bedrocks in the dip slope is loosened by rock creep and is prone to rainwater infiltration. It can be seen that such slopes tend to lead to deep-seated landslides. Therefore, the small drainage density and the small valley erosion index in this area can be one of effective indicators of the destabilizing area.

6. ACKNOWLEDGMENT

We thank the Ministry of Land, Infrastructure, Transport and Tourism Kinki Regional Development Bureau for the providing 5m DEM data of the survey area. And we also thank Dr. Tamotsu Matsui and other related members at the Calamity Science Institute for their valuable discussions.

7. REFERENCES

- Booth, A.M., Roering, J.J., Perron, J.T., 2009. Automated landslide mapping using spectral analysis and high-resolution topographic data: Puget Sound lowlands, Washington, and Portland Hills, Oregon. *Geomorphology*, 109, 132-147.
- Fujisawa, K. and Kasai, Y., 2009. Data Analysis Manual of on Aeronautical Laser Surveying in Landslide Area. *Technical Note of PWRI*, Public Works Research Institute, Tsukuba, JAPAN, No. 4150, 43p.
- Horton, R.E., 1945. Erosional development of streams and their drainage basins: hydrophysical approach to quantitative morphology. *Geological Society of America Bulletin*, 56, 275-370.
- Iwahashi, J., 1994. Development of landform classification using digital elevation model. *Annals of Disaster Prevention Research Institute of Kyoto University*, 37, B-1,141-156.
- Japan Meteorological Agency, 2013. Typhoon Talas relevant information -Portal-. https://www.jma.go.jp/jma/en/typhoon_Talas.html .
- Kinki Regional Development Bureau, Ministry of Land, Infrastructure and Transport, 2013. *Memoir of Disaster Correspondence on 2011 Typhoon Disaster in Kii Peninsula*. Ministry of Land, Infrastructure and Transport, 200p.
- Kishu Shimanto Research Group, 2012. *New Perspective on the study of the Cretaceous to Neogene Shimanto Accretionary Prism in the Kii Peninsula, Southwest Japan*. The Association for the Geological Collaboration in Japan, Monograph 59, 295p.
- NIED, 2005, *Landslide Maps* (1:50000 scale), Vol. 23, Wakayama and Tanabe, 27maps, - Portal-. https://dil-opac.bosai.go.jp/publication/nied_tech_note/landslidemap/pdf-23.html.